

Bound states in the continuum in a fluxonium qutrit

María Hita-Pérez[†], Pedro Orellana[‡], Juan José García-Ripoll[†], Manuel Pino^{*†}

[†] *Institute of Fundamental Physics IFF-CSIC, Calle Serrano 113b, Madrid 28006, Spain*

[‡] *Departamento de Física Universidad Técnica Federico Santa María, Casilla 110-V, Valparaíso, Chile.*

^{*} *Nanotechnology Group, USAL-Nanolab, Universidad de Salamanca, E-37008 Salamanca, Spain.*

The heavy fluxonium at zero external flux has a long-lived state when coupled capacitively to any other system. We analyze it by projecting all the fluxonium relevant operators into the qutrit subspace, as this long-lived configuration corresponds to the second excited fluxonium level. This state becomes a bound-state in the continuum (BIC) when the coupling occurs to an extended system supporting a continuum of modes. In the case without noise, we find BIC decay times that can be much larger than seconds $T_1 \gg s$ when the fluxonium is coupled to a superconducting waveguide, while typical device frequencies are in the order of GHz. We have analyzed different sources of noise in a realistic situation, arguing that the most dangerous one is the well-known $1/f$ flux noise. Even in its presence, BICs decay times could reach the range of $T_1 \sim 10\text{ms}$.

I. INTRODUCTION

Confined quantum excitations generally decay when coupled to a band of states with a continuous spectrum [1]. There are some exceptions to those decay processes where a confined state lying at the continuum part of the spectrum lives forever. Those bound states in the continuum (BICs) were predicted long ago by von Neumann and Wigner [2]. The BICs have appeared on several platforms, some of them following the laws of quantum mechanics as solid-state devices [3–6], some others—under the wave-particle duality—obeying classical wave mechanics [7, 8]. For instances, there have been many studies of BIC's in photonic devices [9–14] since their first experimental observation around ten years ago [15].

There are also proposals to study BICs in high-coherence quantum optical devices. Inspired by the physics of classical BICs with confined electromagnetic fields [16–21], recent works proposed using two-level systems or qubits [22, 23] to create an extremely long-lived and confined single-photon excitation. Another approach based on two-level emitters is to use their collective photon-mediated interactions to create extended BIC states—authors refer to as a multi-dark state—that lives on two or more separated qubits [24].

In this work, we show how to engineer a scalable, compact BIC, using a superconducting circuit, a fluxonium qutrit [25], capacitively embedded in the continuum of microwave excitations from a co-planar waveguide [cf. Fig. 1(a)]. Similar to the classical setup in Ref. [26], where the BIC lives in a photonic resonator connected to an open waveguide, our BIC is the confined plasmonic excitation that lives in the fluxonium loop and is prevented from decaying into the microwave guide. More precisely, the BIC state is the symmetric excited state $|+\rangle$ of the fluxonium potential at zero external flux $\Phi_{\text{ext}} = 0$ [cf. Fig 1(b)]. This state is a BIC state because the $|+\rangle \rightarrow |0\rangle$ transitions are suppressed due to the fact that charge operator is antisymmetric and cannot connect both states, as experimentally observed in Ref. [25]. Moreover, the $|+\rangle \rightarrow |-\rangle$ transition can also be suppressed by a suit-

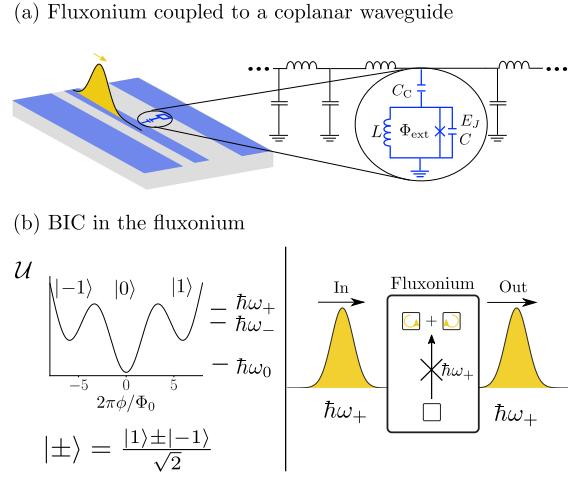


FIG. 1. (a) A fluxonium threaded by an external flux Φ_{ext} is capacitively coupled to a superconducting waveguide. (b) The device potential at $\Phi_{\text{ext}} = 0$ as a function of fluxonium phase ϕ . Its three minima states are denoted by $| -1 \rangle$, $| 0 \rangle$, $| 1 \rangle$. The first and second excited eigenstate of the fluxonium are antisymmetric and symmetric superposition of those states denoted by $| - \rangle$, $| + \rangle$, having each one odd and even parity under fluxonium flux reversal. (c) Due to the odd parity of the capacitive coupling, incoming radiation at the frequency of the $| + \rangle$ state cannot excite this state. This state becomes completely uncoupled from the waveguide if the device capacitance is made large enough.

able choice of the capacitive to inductive energy ratios E_J/E_C , as in capacitively shunted flux qubits [27, 28] and capacitively shunted heavy fluxonium qubits at half frustration [29, 30]. Using these design considerations and realistic parameters, we prove that the BIC can reach very long lifetimes, of order 10ms or greater.

The structure of this work is as follows. We begin with a thorough study of the fluxonium qutrit and the effective capacitive and inductive interactions between the qutrit and external fields. This study reveals a symmetry point at which the $| + \rangle$ state effectively decouples from all external fields. When the fluxonium is placed in a microwave

guide, the capacitive interaction between the qutrit and the propagating fields is described by the effective models we found, and the $|+\rangle$ state becomes a BIC. The lifetime of this state is shown to be extremely long in the presence of realistic $1/f$ flux noise and losses into the dielectric. Finally, we also discuss the implications of these compact BICs for applications in quantum information and quantum sensing, including open questions such as the robust preparation of the $|+\rangle$ in the open system.

II. FLUXONIUM QUTRIT

Let us formalize the intuitive picture of a BIC using a fluxonium circuit. We need to show that a field coupled capacitively to the fluxonium cannot excite transitions in and out of the second excited. This information is obtained from the expansion of the charge operator and the Hamiltonian in the relevant low-energy subspace. This subspace has a qutrit structure, where the BIC mode corresponds to the second excited state, $|+\rangle$. Incidentally, in this qutrit representation of the heavy fluxonium states, flux and charge operators adopt the simple representation of S_x and S_y spin-1 operators, respectively.

A fluxonium [25] consists of a single Josephson junction with Josephson energy E_J shunted by a capacitance C_f and a large inductance L , as shown in Fig. 1(a). The Hamiltonian for such a system is given by:

$$H_f(q, \phi) = \frac{1}{2C_f} q^2 + V(\phi), \text{ with} \\ V(\phi) = \frac{1}{2L} \phi^2 - E_J \cos\left(\frac{\phi + \Phi_{\text{ext}}}{\Phi_0}\right). \quad (1)$$

Here, q is the charge difference on the capacitance, ϕ is the conjugate flux operator, and Φ_{ext} is the external flux passing through the superconducting loop. We typically work at $\Phi_{\text{ext}} = 0$, so that the potential has the shape depicted in 1(b).

The characteristic energies of the fluxonium are the junction's Josephson energy E_J , the charging energy introduced by the capacitance $E_C = e^2/2C_f$, and the inductive energy introduced by the inductance $E_L = (\hbar/2e)^2/L$. The main difference between this and other inductively shunted Josephson junction devices lies precisely in the relation between these parameters, which satisfy $E_L \ll E_J$ and $1 \lesssim E_J/E_C$ [31]. The heavy fluxonium is realized approximately for $E_J/E_C > 5$ [30].

Let us describe an analytical derivation of the qutrit Hamiltonian and relevant operators. At the symmetry point $\Phi_{\text{ext}} = 0$, the potential energy of the fluxonium has two local minima at both sides of the global one. The lowest energy eigenstates around the three minima are denoted $|L\rangle$, $|0\rangle$, $|R\rangle$, as depicted in Fig. 2(a). Intuitively, one would want to use $|L\rangle$, $|0\rangle$, $|R\rangle$ as a qutrit basis. However, the use of the $|L\rangle$ and $|R\rangle$ vectors is problematic in common situations where they have a strong overlap and are close in energy to nearby excitations (thin gray lines in panel (a) of Fig. 2).

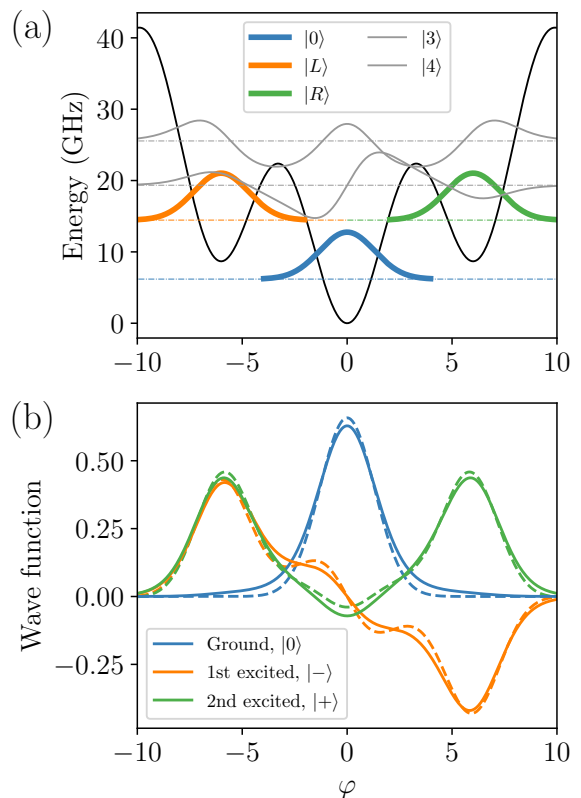


FIG. 2. (a) Potential energy of the fluxonium for $E_J = 10$ GHz, $E_C = 3.6$ GHz and $E_L = 0.46$ GHz [32] as solid black line. Gaussian states in the left $|L\rangle$, center $|0\rangle$ and right $|R\rangle$ wells are denoted with thick solid lines, while thin gray ones are used for third and fourth excited eigenstates. The dashed lines indicate the energy of each of the wavefunctions (Gaussian potential approximation for the Gaussian states). (b) Wavefunction amplitudes of the three lowest eigenstates (solid line) and the approximated ones considering the Gram-Schmidt orthogonalization up to the 4th excited state (dashed line).

One solution is to replace the $|L\rangle$ and $|R\rangle$ states with slightly modified vectors that have been orthogonalized with respect to other low-energy excitations. Fig. 2(b) compares the exact eigenstates (solid lines) of a fluxonium with intermediate values of E_J/E_C together with the approximated eigenstates (dashed lines) computed with a Gram-Schmidt orthogonalization up to the 4th excited state. The agreement is good, and helps in capturing the part of the excited wavefunction that tunnels to intermediate region $\varphi \simeq 0$, a feature that is not present in the original intuitive expansion. Moreover, these features introduce relevant qutrit interactions terms that are mediated by higher energy excitations.

To keep computations tractable, we can orthogonalize the $|L\rangle$ and $|R\rangle$ states with respect to just the third excited state $|-1\rangle = \frac{|L\rangle - a|3\rangle}{\sqrt{1-a^2}}$ and $|1\rangle = \frac{|R\rangle + a|3\rangle}{\sqrt{1-a^2}}$, parameterizing the overlap with a new parameter $a = \langle 3|L\rangle = -\langle 3|R\rangle$. We will verify that this order of perturbation

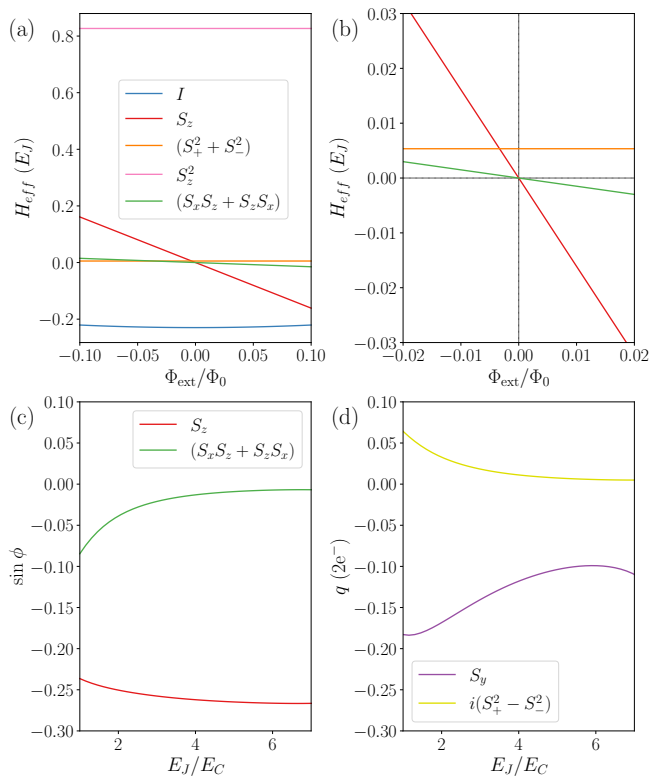


FIG. 3. (a) Effective Hamiltonian of a fluxonium qutrit with $E_J/E_C = 2.78$ and $E_J/E_L = 21.74$ [33] as a function of the external flux (Φ_{ext}). Panel (b) is a zoom near the origin. Effective flux sine $\sin \phi$ (c) and charge q (d) operators for the fluxonium with $E_J/E_L = 21.74$ as a function of E_J/E_C .

is sufficient to recover the qualitative form of the qutrit operators. Let us denote by $\pm\phi_*$ the position of the local minima in units of flux, and assume that the capacitance of the fluxonium is large enough to prevent direct tunneling between them $\langle L|R \rangle = \langle L|0 \rangle = \langle R|0 \rangle \approx 0$. The projection of the flux operator and of the Hamiltonian onto the qutrit spin-1 base then reads:

$$\phi = \tilde{\phi}_* S_z + b(S_x S_z + S_z S_x), \quad (2)$$

$$H = \epsilon S_z^2 + \frac{\Delta}{2}(S_+^2 + S_-^2) + \Phi_{\text{ext}} J_0 \sin(\phi). \quad (3)$$

Here, E_3 is the eigenenergy of the third excited state, $\tilde{\phi}_* = \frac{1-2a^2}{1-a^2}\phi_*$, $b = \frac{\sqrt{2}a}{\sqrt{1-a^2}}\langle 0|\phi|3 \rangle$ and $\Delta = \frac{E_3 a^2}{1-a^2}$ with $\epsilon = \mathcal{U}(\phi_*)$. Last but not least, we can compute the fluxonium charge operator acting on the qutrit subspace as in Ref. [27], via the Heisenberg equation $q = \frac{iC_f}{\hbar}[H, \phi]$:

$$q = \frac{iC_f}{\hbar} \left[ib(\epsilon - \Delta) S_y + \Delta \tilde{\phi}_* (S_+^2 - S_-^2) \right]. \quad (4)$$

Our derivation expresses all operators in terms of the overlap a and the energy E_3 , quantities that may be estimated using the harmonic states of the right, left, and central wells. Intuitively, all terms containing a in Eqs. (3)-(4) are mediated by the third excited state. In

the limit of large charging capacitance or *heavy fluxonium*, the $|-1\rangle, |1\rangle, |0\rangle$ states become strongly localized in left, center, and right well, making the factor a exponentially small. In this case, the charge and flux operators converge respectively to S_y and S_z (notice the large factor ϵ in front of S_y in the q expansion), and the Hamiltonian is diagonalized by the states $|0\rangle$ and $|\pm\rangle = [|L\rangle \pm |R\rangle]/\sqrt{2}$ at zero bias $\Phi_{\text{ext}} = 0$. As explained in the introduction, in this limit the charge operator $q \approx S_y$ cannot mediate the decay of the $|+\rangle$ state to the ground state $|0\rangle$, and the second excited state can be used to construct a BIC.

We have compared the analytical estimates with numerical diagonalizations, obtaining an excellent qualitative agreement. In our method we compute the lowest energy eigenstates, project the relevant operators onto the qutrit basis and express them as combination of 1-spin operators. For greater accuracy, we use the $\sin(\phi)$ operator instead of ϕ , and recover this and the q operator as derivatives of the fluxonium's Hamiltonian with respect to flux and voltage perturbations, respectively. We use some of the subroutine of CircuitQ library [34] and our own code.

Fig. 3 illustrates the excellent agreement between our predictions Eqs. (3)-(4), and the expansions of the Hamiltonian as a function of external magnetic flux $\Phi_{\text{ext}} = 0$ (a-b), and of the flux (c) and charge (d) as a function of E_J/E_C at $\Phi_{\text{ext}} = 0$. Following our previous discussion, we see that charge and flux effectively become S_x, S_y with other terms exponentially vanishing with increasing fluxonium capacitance. Knowing that at zero flux the second excited state is $|+\rangle$, we have obtained rigorously that the matrix element of this state with the other qutrit state is suppressed exponentially fast for the heavy fluxonium. This state becomes a BIC when the fluxonium is coupled via its charge operator to an extended object with a continuous spectrum, as we show next.

III. BIC IN A FLUXONIUM QUTRIT COUPLED TO A WAVEGUIDE

Let us now discuss the dynamics of a fluxonium with a capacitive coupling C_c to the continuum of propagating modes in a coplanar microwave guide, as shown in Fig. 4(a). From quantum optical considerations, the waveguide is a gapless medium supporting frequencies that would allow the fluxonium qubit to relax and decay from the $|+\rangle$ to the $|0\rangle$ or $|-\rangle$ states. However, based on our study of the charge operator, we conclude that the decay rate $\Gamma_{+0} = 0$ because of symmetry considerations, and that Γ_{+-} becomes vanishingly small with increasing fluxonium capacitance. In this limit, at zero bias the $|+\rangle$ state becomes a quasi-BIC state with an exponentially long lifetime [35].

To compute the BIC's lifetime we use the spin-boson model [36] for a fluxonium at the middle of a $\lambda/2$ -

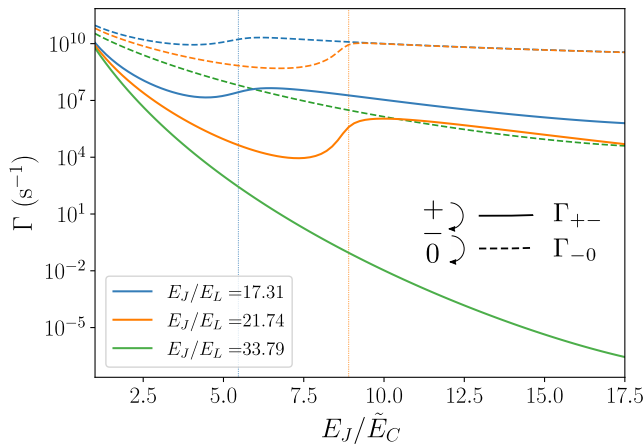


FIG. 4. Transition rates for the allowed transitions in the fluxonium qutrit as a function of the ratio between Josephson and renormalized charging energies, $\tilde{E}_C = \frac{e^2}{2C_\Sigma}$. The transition rates from the BIC state $|+\rangle$ to $|-\rangle$ appears as solid lines and from the $|-\rangle$ to $|0\rangle$ as dashed lines. The Josephson energy of the fluxonium is $E_J = 10\text{GHz}$ and the linear inductances are chosen so that they are experimentally realizable $E_J/E_L = 17.31$ [25], $E_J/E_L = 21.74$ [32] and $E_J/E_L = 33.79$ [29]. The waveguide has impedance $\mathcal{Z} = 50\Omega$ and the coupling capacitance is taken $(E_C)_c = 0.25\text{GHz}$. The vertical dashed lines indicate the the value of \tilde{E}_C at which there is an avoided level crossing in the fluxonium spectrum between the second and third excited states.

waveguide of length L [37, 38]:

$$H = \frac{1}{2C_\Sigma} q^2 + V(\phi) + \sum_{n=0}^{N-1} \hbar\omega_n \left(b_n^\dagger b_n + \frac{1}{2} \right) + \Delta H$$

$$\Delta H = \frac{C_c}{C_\Sigma} q \sum_{n=0}^{N-1} (-1)^n \sqrt{\frac{\hbar\omega_n}{2c_0 L}} i(b_n - b_n^\dagger). \quad (5)$$

We have expanded the waveguide Hamiltonian using the normal modes $[b_n, b_m] = i\hbar\delta_{n,m}$ with $n, m = 0, \dots, N-1$, introducing waveguide's capacitance per unit length $c_0 = C/L$ and the renormalized fluxonium's capacitance $C_\Sigma = C_f + C_c$.

Fermi's Golden Rule [39] is a good estimate for the transition rates Γ_{ij} between fluxonium states i and j assisted by the modes of the waveguide. The formula requires the interaction Hamiltonian ΔH and the density of states $\rho(\omega)$ which, for a waveguide with a linear dispersion relation $\omega = \nu k$, is uniform $\rho(\omega) = L/(2\pi\nu)$. In this case Fermi's Golden Rule (see [40] for an inductive coupling) predicts:

$$\Gamma_{ij} = 2\pi \left(\frac{C_c}{C_\Sigma} \right)^2 G_0 \mathcal{Z} |\langle i|N_f|j\rangle|^2 \omega_{ij}, \quad (6)$$

as a function of the transition frequency ω_{ij} , the number of Cooper pairs in the fluxonium $N_f = q/2e$ and the line's impedance $\mathcal{Z} = c_0\nu$. As discussed, direct transitions

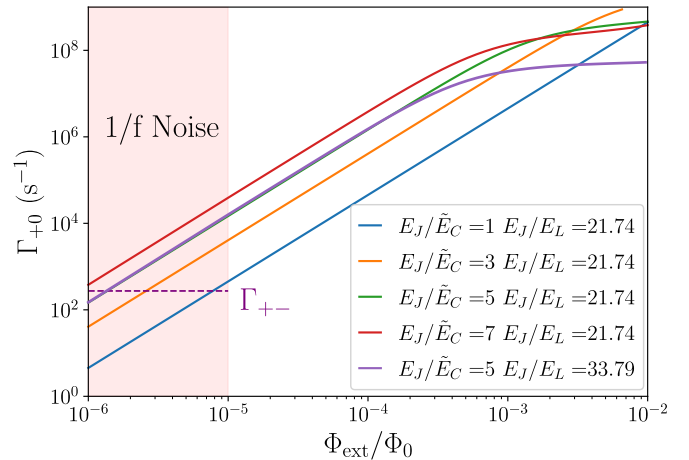


FIG. 5. Transition rate from $|+\rangle$ to $|0\rangle$ due to radiative losses of the waveguide as a function of the external flux, Φ_{ext} , in log-log scale. The Josephson energy of the fluxonium is $E_J = 10\text{GHz}$. The waveguide has impedance $\mathcal{Z} = 50\Omega$ and the coupling capacitance is taken $(E_C)_c = 0.25\text{GHz}$. The dashed line signals the transition rate $\Gamma_{+-} \approx 3 * 10^2\text{Hz}$ for the fluxonium parameters of the purple line $E_J/\tilde{E}_C = 5$ and $E_J/E_L = 33.79$. (see Fig. 4). The pink coloured region signals the typical amplitudes of quasi-static fluctuations in fluxoniums produced by $1/f$ noise.

from $|+\rangle \rightarrow |0\rangle$ are forbidden by symmetry $\Gamma_{+0} = 0$, and the $|+\rangle$ state can decay only via the $|-\rangle$ state.

Fig. 4 displays the transition rates from the $|+\rangle$ to the $|-\rangle$ states (solid lines), as computed numerically using the Fermi Golden Rule and the exact eigenstates of the model. The parameters for each data set corresponds to each of the experiments in Refs. [25, 29, 32]. The ideal lifetime of the BIC—the inverse of this relevant transition rate $T_{\text{BIC}} \approx 1/\Gamma_{+-}$ —is exponentially enhanced as we increase the renormalized charging energy of the fluxonium \tilde{E}_C . The other relevant transition rate in the qutrit subspace Γ_{-0} (dashed line) decreases much slower than Γ_{+-} , meaning that only the $+$ states is uncoupled from the waveguide.

It is important to remark that for certain parameters, the energy of the third excited state $|3\rangle$ approaches the qutrit subspace and breaks all our approximations. As shown by the orange curve in Fig. 4, this manifests as a change in tendency in the decay rates, at a point where the BIC state ceases to exist. The value of E_J/\tilde{E}_C at which this happens depends strongly on the ratio E_J/E_L . This value determines the gap between the qutrit subspace and the high energy levels and sets a limit to the experimentally achievable lifetime of the BIC $|+\rangle$ state. However, as also shown in Fig. 4, appropriately tuning the ratio of inductive energies, such as $E_J/E_L = 33.79$ with $E_J = 10\text{GHz}$, yields lifetimes that are exponentially large, above $T_1 \gg s$, justifying that we call the $|+\rangle$ state a BIC.

Rigorously, the symmetry that protects the BIC state only appears for integer flux values $\Phi_{\text{ext}} = \Phi_0 \times \mathbb{Z}$. Mov-

ing away from this limit activates $\Gamma_{+0} \neq 0$ and the lifetime of the quasi-BIC state is strongly reduced. This harmful mechanism is present for all types of flux noise, even quasi-static one—i.e. fluctuations of the flux that remain approximately constant over a single iteration of the experiment. However, we argue that (i) the lifetime reduction due to standard flux noise is sufficiently small and (ii) using flux biases may be an interesting way to remove the protection and actually populate the BIC state.

To understand this, we rely on state-of-the-art models for how low-frequency flux noise penetrates Josephson devices in quantum information applications [41–43]. This noise has a power spectrum that can be approximated as $S(\omega) \sim 2\pi A^2/\omega$ with $A \approx (10^{-5} - 10^{-6})\Phi_0$ [44–47], which implies quasi-static fluctuations with an amplitude $\sigma \sim (10^{-5} - 10^{-6})\Phi_0$ (see Supplemental Material). Fig. 5 displays the transition rate from the BIC to the ground state as a function of the flux deviation $\Phi_{\text{ext}} \neq 0$. Using perturbation theory, we obtain $\Gamma_{+0} \sim (E_J/E_C)^2 \Phi_{\text{ext}}^2$. This dependence is reflected in Fig. 5 where in log-log scale all curves share the slope of this quadratic dependency. This figure also confirms that the BIC becomes more sensitive to external flux perturbations as the ratio E_J/E_C is increased. As commented before, we expect low-frequency flux fluctuations with amplitude $10^{-5} - 10^{-6}\Phi_0$, denoted by a colored region in Fig. 5. In this region the noise-induced decay Γ_{+0} can grow substantially, unless we make a "not too heavy" fluxonium.

As example of a realistic compromise that works well for a pessimistic estimate of fluctuations $\sim 10^{-5}\Phi_0$, the purple line from Fig. 5 $\frac{E_J}{E_C} \approx 5$, $\frac{E_J}{E_L} \approx 30$, produces a BIC with a decay time $T_1 \sim 10^{-1}$ ms, where the contribution of $\Gamma_{+-} \approx 2 * 10^{-2}$ s is small [cf. horizontal dashed line in Fig. 5]. For a moderately optimistic noise amplitude $\sim 10^{-6}\Phi_0$, a BIC with the same parameters would produce an expected decay time of $T_1 \sim 10$ ms, as now the radiative losses due to the $|+\rangle \rightarrow |0\rangle$ and $|+\rangle \rightarrow |-\rangle$ are of the same order.

When the influence of $1/f$ noise is small, there are other noise sources that need to be considered. In this limit, losses into the dielectric [48] may become the most important decay channel. This has been demonstrated in Ref. [47] for some fluxonium qubits, where a detailed characterization of dielectric losses showed that they were the dominant decay channel, giving relaxation times $\sim 10^{-1}$ ms. In our setup, the $|+\rangle \rightarrow |-\rangle$ decay channel could be enabled by matrix elements in the flux operator that couple to high-frequency currents in the dielectric [49]. While we cannot provide ab-initio estimates of this relaxation channel, we can extrapolate the scaling of the decay time, which—as shown in Supplemental Material and Ref. [47]—scales quadratically $\Gamma_{\text{diel}} \sim \omega_{+-}^\beta$ ($\beta \approx 2$) as a function of the separation between excited states ω_{+-} . By working closer to the heavy fluxonium limit, both ω_{+-} and the decay rate can be significantly reduced. This way, we expect that we can improve the lifetime of the BIC, up from $T_1 \approx 100\mu\text{s}$ for the fluxonium in Ref. [47], up to a lifetime that is closer to the $1/f$ -limited

lifetimes discussed above, $T_1 \sim 10$ ms (see Supplemental Material).

IV. CONCLUSIONS

In summary, in this work, we have shown how to construct a compact BIC living in a superconducting fluxonium qubit that is capacitively connected to an open microwave guide. Furthermore, we have found that this device can be brought to a regime where the second excited state is a quasi-BIC state. That is a state with a highly long decay time that, under realistic parameters devices, can reach up to tens of milliseconds. The key ingredient for the BIC is the destructive quantum interference between opposite persistent current states that appears at $\Phi_{\text{ext}} = 0$ [26]. As a result, we have a fully tunable BIC that can be brought in and out of the protected state just by tuning the magnetic field in its loop.

The possibility of creating long-lived BIC states in small fluxonium devices is exciting as a scalable platform for storing protected quantum information. However, as discussed above, there is a compromise between the lifetime of the BIC state and the possibility of accessing those states using external fields. It, therefore, remains an open question of how to scalably and coherently prepare these states in realistic setups. Some avenues that can be explored with the tools developed in this work include the engineering of $|+\rangle$ states by dynamically tuning the external magnetic fields and controlling the injection of photons or using multi-photon induced transitions via excited states.

We have also shown that the fluxonium BIC configuration is very sensitive to external magnetic fields. In particular, we believe that it is possible to build a magnetic field sensor by monitoring the $|+\rangle \leftrightarrow |0\rangle$ resonance, as both the intensity and linewidth of that resonance depend on small deviations of the magnetic flux experienced by the fluxonium [cf. Fig. 5]. For instances, a change in magnetic field of $\Delta B = 10$ nT would produce a change in the magnetic flux of a typical fluxonium (area $\sim 10^3\mu\text{m}^2$) of $\Delta\Phi \approx 5 * 10^{-3}\Phi_0$, which activates the BIC. The activation associated with the excess of magnetic field can then be recorded in the measurements of the resonance. We believe that this method could be competitive when compared with others, as the ones based on nitrogen-vacancy centers [50].

ACKNOWLEDGMENTS

This work is supported by the European Commission FET-Open project AVaQus GA 899561, by Proyecto Sinérgico CAM 2020 Y2020/TCS-6545 (NanoQuCoCM) and CSIC Quantum Technologies Platform PTI-001. We acknowledge Centro de Supercomputación de Galicia (CESGA) who provided access to the supercomputer FinisTerae for performing simulations.

Part of the simulations were performed on the Tirant node of the Red de Española de Supercomputación (RES). M. P. acknowledges support by Spanish MCIN/AEI/10.13039/501100011033 through Grant No. PID2020-114830GB-I0.

Appendix A: Quasi-Static noise

Typical flux fluctuations for a fluxonium device can be extracted from its noise power spectrum. We are interested in the low-frequency flux noise, which can bias the device for long enough time and, thus, produce a decay of the BIC into the waveguide. The dominant source of low-frequency flux noise in the type of devices treated here is the one referred as $1/f$ noise, so it is important to understand its properties in order to characterize BIC decay in realistic situations.

We assume a power spectrum as explained in the Appendix of Ref. [47], based on many previous experimental results:

$$S(\omega) = 2\pi A^2/\omega$$

with $A = (10^{-5} - 10^{-6})\Phi_0$. We set a low and high frequency cut-off for the $1/f$ noise as $\gamma_- = 10^{-2}\text{Hz}$ and $\gamma_+ = 10^1\text{Hz}$, which is consistent with the experimental results in Ref. [45] (red points in Fig. 3 of that reference). We will see that, in any case, the values of those cut-offs do not affect that much the final results.

Once the noise model is set, we can extract the fluctuations at the low frequency cut-off, the important one for the BIC, as the real part of the Fourier transform of the power spectrum:

$$\sigma^2 \approx \langle \Phi_{\text{ext}}(t)\Phi_{\text{ext}}(t + \tau) \rangle = A^2 \int_{\gamma_-}^{\gamma_+} \frac{d\omega}{\omega} \cos(\omega\tau). \quad (\text{A1})$$

The time $\tau \sim 1/\gamma_-$ should be of the order of the inverse of the low-frequency cut-off so to get the amplitude of the quasi-static fluctuations. Setting this value in the previous formula, we obtain:

$$\sigma^2 \approx A^2 \int_1^{\frac{\gamma_+}{\gamma_-}} \frac{dx}{x} \cos(x). \quad (\text{A2})$$

Expressing the previous results in terms of the cosine integral function

$$\text{Ci}(x) = - \int_x^\infty \frac{dx}{x} \cos(x), \quad (\text{A3})$$

and taking $\frac{\gamma_+}{\gamma_-} = 10^3$ we get the desired amplitude as given by:

$$\sigma^2 = A^2 [-\text{Ci}(10^3) + \text{Ci}(1)] \sim \mathcal{O}(1)A^2. \quad (\text{A4})$$

As we previously state, this result do not depend strongly on the low and high-energy cut-offs as $|\text{Ci}(x)| < 1/x$ vanishes fast. For our purposes, we take $\sigma \approx A$, because the factor of order one is irrelevant due to the uncertainty in the magnitude A itself. Thus, we have taken the fluctuations in Fig. (4) of the main text as given by $A = (10^{-5} - 10^{-6})\Phi_0$.

Appendix B: Dielectric noise

It is argued in Ref. [47], that the main source of relaxation in the fluxonium qubit is tangential losses into the dielectric. Those losses have been shown to be an important source of dissipation for several devices, such as phase qubits or transmons [48, 51]. We can extract the decay time using the phenomenological model found in Ref. [47] for the fluxonium, but now describing the transition from the BIC to the $-$ state:

$$\Gamma = |\varphi_{+-}|^2 \frac{\hbar\omega_{+-}^2}{8E_C} \left(\frac{\omega_{+-}}{12\pi\text{GHz}} \right)^\gamma \left(\coth \left(\frac{\hbar\omega_{+-}}{2k_bT} \right) + 1, \right)$$

with $\gamma \approx 0.15$ and $\varphi_{+-} \sim |\langle -|\varphi|+ \rangle|$. The experimental results validated this law, giving decay times around $T_1 \sim 100\mu\text{s}$ at the sweet spot for direct transitions from the $1 \rightarrow 0$, where $E_{01} \approx 0.8\text{GHz}$. We notice that for the parameters we have seen that the fluxonium BIC has a large decay time $\frac{E_J}{E_C} \approx 5$, $\frac{E_J}{E_L} \approx 30$, the energy of the relevant transition has an small frequency $E_{+-} \sim 0.01\text{GHz}$, much smaller that the one for the qubit transition. Taking into account that the transition rate depends almost quadratically in the previous equation, we expect a rough increase of the decay time by, at least, three orders of magnitude for the decay of the BIC due to dielectric losses BIC $T_1 \approx 10^{-2}\text{s}$. We conclude that this source of noise should not affect to the BIC stability.

-
- [1] P. A. M. Dirac, The quantum theory of the emission and absorption of radiation, Proceedings of the Royal Society of London. Series A, Containing Papers of a Mathematical and Physical Character **114**, 243 (1927).
 [2] J. von Neumann and E. P. Wigner, Über das Verhalten von eigenwerten bei adiabatischen prozessen, in *The Collected Works of Eugene Paul Wigner* (Springer, 1993) pp.

- 294–297.
 [3] F. Capasso, C. Sirtori, J. Faist, D. L. Sivco, S.-N. G. Chu, and A. Y. Cho, Observation of an electronic bound state above a potential well, Nature **358**, 565 (1992).
 [4] J. P. Ramos-Andrade, D. Zambrano, and P. A. Orellana, Fano-majorana effect and bound states in the continuum on a crossbar-shaped quantum dot hybrid structure, An-

- nalén der Physik **531**, 1800498 (2019).
- [5] M. L. De Guevara and P. Orellana, Electronic transport through a parallel-coupled triple quantum dot molecule: Fano resonances and bound states in the continuum, *Physical Review B* **73**, 205303 (2006).
 - [6] J. González, M. Pacheco, L. Rosales, and P. Orellana, Bound states in the continuum in graphene quantum dot structures, *EPL (Europhysics Letters)* **91**, 66001 (2010).
 - [7] R. Parker, Resonance effects in wake shedding from parallel plates: some experimental observations, *Journal of Sound and Vibration* **4**, 62 (1966).
 - [8] R. Parker, Resonance effects in wake shedding from parallel plates: calculation of resonant frequencies, *Journal of Sound and Vibration* **5**, 330 (1967).
 - [9] S. Weimann, Y. Xu, R. Keil, A. E. Miroshnichenko, A. Tünnermann, S. Nolte, A. A. Sukhorukov, A. Szameit, and Y. S. Kivshar, Compact surface fano states embedded in the continuum of waveguide arrays, *Physical review letters* **111**, 240403 (2013).
 - [10] G. Corrielli, G. Della Valle, A. Crespi, R. Osellame, and S. Longhi, Observation of surface states with algebraic localization, *Physical review letters* **111**, 220403 (2013).
 - [11] Y. Yang, C. Peng, Y. Liang, Z. Li, and S. Noda, Analytical perspective for bound states in the continuum in photonic crystal slabs, *Physical review letters* **113**, 037401 (2014).
 - [12] A. I. Ovcharenko, C. Blanchard, J.-P. Hugonin, and C. Sauvan, Bound states in the continuum in symmetric and asymmetric photonic crystal slabs, *Physical Review B* **101**, 155303 (2020).
 - [13] A. Kodigala, T. Lepetit, Q. Gu, B. Bahari, Y. Fainman, and B. Kanté, Lasing action from photonic bound states in continuum, *Nature* **541**, 196 (2017).
 - [14] Z. Yu and X. Sun, Acousto-optic modulation of photonic bound state in the continuum, *Light: Science & Applications* **9**, 1 (2020).
 - [15] Y. Plotnik, O. Peleg, F. Dreisow, M. Heinrich, S. Nolte, A. Szameit, and M. Segev, Experimental observation of optical bound states in the continuum, *Physical review letters* **107**, 183901 (2011).
 - [16] H. Dong, Z. R. Gong, H. Ian, L. Zhou, and C. P. Sun, Intrinsic cavity qed and emergent quasinormal modes for a single photon, *Phys. Rev. A* **79**, 063847 (2009).
 - [17] T. Tufarelli, F. Ciccarello, and M. Kim, Dynamics of spontaneous emission in a single-end photonic waveguide, *Physical Review A* **87**, 013820 (2013).
 - [18] T. Tufarelli, M. Kim, and F. Ciccarello, Non-markovianity of a quantum emitter in front of a mirror, *Physical Review A* **90**, 012113 (2014).
 - [19] I.-C. Hoi, A. F. Kockum, L. Tornberg, A. Pourkabirian, G. Johansson, P. Delsing, and C. Wilson, Probing the quantum vacuum with an artificial atom in front of a mirror, *Nature Physics* **11**, 1045 (2015).
 - [20] M. Cotrufo and A. Alù, Excitation of single-photon embedded eigenstates in coupled cavity-atom systems, *Optica* **6**, 799 (2019).
 - [21] L. Zhou, Z. R. Gong, Y.-x. Liu, C. P. Sun, and F. Nori, Controllable scattering of a single photon inside a one-dimensional resonator waveguide, *Phys. Rev. Lett.* **101**, 100501 (2008).
 - [22] G. Calajó, Y.-L. L. Fang, H. U. Baranger, F. Ciccarello, *et al.*, Exciting a bound state in the continuum through multiphoton scattering plus delayed quantum feedback, *Physical review letters* **122**, 073601 (2019).
 - [23] A. Feiguin, J. J. García-Ripoll, and A. González-Tudela, Qubit-photon corner states in all dimensions, *Physical Review Research* **2**, 023082 (2020).
 - [24] M. Zanner, T. Orell, C. M. Schneider, R. Albert, S. Oleschko, M. L. Juan, M. Silveri, and G. Kirchmair, Coherent control of a multi-qubit dark state in waveguide quantum electrodynamics, *Nature Physics* , 1 (2022).
 - [25] V. E. Manucharyan, J. Koch, L. I. Glazman, and M. H. Devoret, Fluxonium: Single cooper-pair circuit free of charge offsets, *Science* **326**, 113 (2009).
 - [26] M. Ahumada, P. Orellana, and J. Retamal, Bound states in the continuum in whispering gallery resonators, *Physical Review A* **98**, 023827 (2018).
 - [27] M. Hita-Pérez, G. Jaumà, M. Pino, and J. J. García-Ripoll, Ultrastrong capacitive coupling of flux qubits, *Physical Review Applied* **17**, 014028 (2022).
 - [28] M. Hita-Pérez, G. Jaumà, M. Pino, and J. J. García-Ripoll, Three-josephson junctions flux qubit couplings, *Applied Physics Letters* **119**, 222601 (2021).
 - [29] N. Earnest, S. Chakram, Y. Lu, N. Irons, R. K. Naik, N. Leung, L. Ocola, D. A. Czaplewski, B. Baker, J. Lawrence, *et al.*, Realization of a λ system with metastable states of a capacitively shunted fluxonium, *Physical review letters* **120**, 150504 (2018).
 - [30] H. Zhang, S. Chakram, T. Roy, N. Earnest, Y. Lu, Z. Huang, D. K. Weiss, J. Koch, and D. I. Schuster, Universal fast-flux control of a coherent, low-frequency qubit, *Phys. Rev. X* **11**, 011010 (2021).
 - [31] M. Peruzzo, F. Hassani, G. Szep, A. Trioni, E. Redchenko, M. Žemlička, and J. Fink, Geometric superinductance qubits: Controlling phase delocalization across a single josephson junction, *arXiv preprint arXiv:2106.05882* (2021).
 - [32] U. Vool, I. M. Pop, K. Sliwa, B. Abdo, C. Wang, T. Brecht, Y. Y. Gao, S. Shankar, M. Hatridge, G. Catelani, *et al.*, Non-poissonian quantum jumps of a fluxonium qubit due to quasiparticle excitations, *Physical review letters* **113**, 247001 (2014).
 - [33] U. Vool, A. Kou, W. Smith, N. Frattini, K. Serniak, P. Reinhold, I. Pop, S. Shankar, L. Frunzio, S. Girvin, *et al.*, Driving forbidden transitions in the fluxonium artificial atom, *Physical Review Applied* **9**, 054046 (2018).
 - [34] P. Aumann, T. Menke, W. D. Oliver, and W. Lechner, Circuitq: An open-source toolbox for superconducting circuits, *arXiv preprint arXiv:2106.05342* (2021).
 - [35] We use the term *quasi-BIC* to indicate that the BIC state has always a finite lifetime.
 - [36] M. Pino and J. J. García-Ripoll, Quantum annealing in spin-boson model: from a perturbative to an ultrastrong mediated coupling, *New Journal of Physics* **20**, 113027 (2018).
 - [37] J. J. Garcia-Ripoll, B. Peropadre, and S. De Liberato, Light-matter decoupling and a2 term detection in superconducting circuits, *Scientific reports* **5**, 1 (2015).
 - [38] A. Parra-Rodriguez, E. Rico, E. Solano, and I. Egusquiza, Quantum networks in divergence-free circuit qed, *Quantum Science and Technology* **3**, 024012 (2018).
 - [39] D. J. Griffiths, *Introduction to quantum mechanics* (Pearson International Edition (Pearson Prentice Hall, Upper Saddle River, 2005), 1962).
 - [40] I. Moskalenko, I. Besedin, I. Simakov, and A. Ustinov, Tunable coupling scheme for implementing two-qubit gates on fluxonium qubits, *Applied Physics Letters* **119**, 194001 (2021).

- [41] R. H. Koch, J. Clarke, W. Goubau, J. M. Martinis, C. Pegrum, and D. J. Van Harlingen, Flicker ($1/f$) noise in tunnel junction dc squids, *Journal of low temperature physics* **51**, 207 (1983).
- [42] R. C. Bialczak, R. McDermott, M. Ansmann, M. Hofheinz, N. Katz, E. Lucero, M. Neeley, A. D. O'Connell, H. Wang, A. N. Cleland, and J. M. Martinis, $1/f$ flux noise in josephson phase qubits, *Phys. Rev. Lett.* **99**, 187006 (2007).
- [43] E. Paladino, Y. M. Galperin, G. Falci, and B. L. Altshuler, $1/f$ noise: Implications for solid-state quantum information, *Rev. Mod. Phys.* **86**, 361 (2014).
- [44] R. H. Koch, D. P. DiVincenzo, and J. Clarke, Model for $1/f$ flux noise in squids and qubits, *Physical review letters* **98**, 267003 (2007).
- [45] F. Yan, S. Gustavsson, A. Kamal, J. Birenbaum, A. P. Sears, D. Hover, T. J. Gudmundsen, D. Rosenberg, G. Samach, S. Weber, *et al.*, The flux qubit revisited to enhance coherence and reproducibility, *Nature communications* **7**, 1 (2016).
- [46] P. Kumar, S. Sendelbach, M. A. Beck, J. W. Freeland, Z. Wang, H. Wang, C. C. Yu, R. Q. Wu, D. P. Pappas, and R. McDermott, Origin and reduction of $1/f$ magnetic flux noise in superconducting devices, *Phys. Rev. Applied* **6**, 041001 (2016).
- [47] L. B. Nguyen, Y.-H. Lin, A. Somoroff, R. Mencia, N. Grabon, and V. E. Manucharyan, High-coherence fluxonium qubit, *Physical Review X* **9**, 041041 (2019).
- [48] J. M. Martinis, Surface loss calculations and design of a superconducting transmon qubit with tapered wiring, *npj Quantum Information* **8**, 1 (2022).
- [49] This noise cannot produce decay from $|+\rangle$ to $|0\rangle$ as they have equal parity.
- [50] A. Kuwahata, T. Kitaizumi, K. Saichi, T. Sato, R. Igarashi, T. Ohshima, Y. Masuyama, T. Iwasaki, M. Hatano, F. Jelezko, *et al.*, Magnetometer with nitrogen-vacancy center in a bulk diamond for detecting magnetic nanoparticles in biomedical applications, *Scientific reports* **10**, 1 (2020).
- [51] J. M. Martinis, K. B. Cooper, R. McDermott, M. Steffen, M. Ansmann, K. Osborn, K. Cicak, S. Oh, D. P. Pappas, R. W. Simmonds, *et al.*, Decoherence in josephson qubits from dielectric loss, *Physical review letters* **95**, 210503 (2005).